Recovery and recrystallization in the superplastic deformation of AA5182

Chen, Z.; Kazantzis, A. V.; De Hosson, J. Th. M.

Published in:
Materialwissenschaft und Werkstofftechnik

DOI:
10.1002/mawe.200800289

 DOI: 10.1002/mawe.200800289

Recovery and recrystallization in the superplastic deformation of AA5182

Z. Chen, A.V. Kazantzis, J.Th.M. De Hosson

The coarse-grained Al alloy AA5182 exhibits poor superplasticity with a maximum elongation to failure not exceeding 220 % at 450 °C and at 10^{-2} s^{-1}. The low values of the strain rate sensitivity indicate that the dislocation velocity is quite high and necking is developed quite soon during extension. The size (often exceeding 1 μm) and the distribution of the precipitates render them incapable of pinning the subgrain boundaries efficiently. As a result recovery and reconstruction by grain refinement occurs only within the necking region where the applied stress is concentrated. A fabrication method which will be able to introduce a large number of submicron sized precipitates will most likely result in sufficient pinning of the subgrain boundaries. This will promote recovery and reconstruction to take place more uniformly in the material rendering it appreciably superplastic.

Keywords: Recovery, recrystallization, superplastic, deformation

1 Introduction

Conventional superplasticity in Al-Mg alloys is carried out by a deformation mechanism based on grain boundary sliding. This mechanism requires fine, stable grain sizes of the order of 10 μm [1–3]. The main limitation of these alloys is the high forming time, which is associated with strain rates generally lower than 10^{-3} s^{-1}, because grain boundary sliding requires accommodation by diffusion controlled mechanisms, i.e. dislocation climb [4], which result in a strain rate sensitivity of the order of 0.5.

A decrease in the forming time can be obtained using coarse-grained Al-Mg alloys which present high ductility at strain rates of the order of 10^{-2} s^{-1}, or higher [5]. The mechanism of coarse-grained superplasticity, also been referred to as "enhanced ductility" or "quasi-superplasticity" [6–7], is characterized by low flow stress and is mainly based on solute drag creep [8]. This mechanism has virtually no grain size dependence, and therefore, the preparation of these materials is less elaborate and thus less costly. The superplastic deformation of coarse-grained materials at high temperatures, however, cannot be considered solely on the basis of the solute drag creep, because it is accompanied by dynamic recovery and recrystallization. The microstructure undergoes extensive modification and shows less and less resemblance to the original. Dynamic recovery and/or reconstruction is often demonstrated by extensive grain refinement, which is attributed to the formation of subgrain boundaries and their conversion into low-angle and high-angle grain boundaries. These, as well as dynamic recrystallization alter the microstructure so that grain size dependent and grain size independent mechanisms occur concurrently [9]. The strain rate sensitivity, which affects the necking instability, is close to 0.3 and thus at these strain rate regimes, coarse grained materials are expected to exhibit lower values of maximum tensile elongation.

The AA5182 Al-Mg alloy is less costly than AA5083 and may prove to be a suitable candidate for the transition of the automotive industry from niche applications, where conventional superplastic forming of fine-grained alloys is used, towards volume component production. In the present study we focus on the mechanical behavior and microstructure evolution of a coarse-grained and a conventional AA5182 Al-Mg alloy. First the optimum deformation conditions are determined, i.e. the strain rate and the temperature, where the maximum tensile elongation is observed and then Orientation Imaging Microscopy – Electron Backscattered Diffraction (OIM - EBSD) is employed to characterize the evolution of the microstructure at these conditions.

2 Experimental procedure

The material used in this study is AA5182, with composition Al – 5.0 % Mg – 0.25 % Mn — 0.10 % Cu (in wt. %) and impurities of Fe (≈ 0.15 %), Si (< 0.15 %) and traces of Cr. The average grain size of the as-received coarse-grained material (henceforth denoted as material C) was 34 μm, whereas that of the conventional material (henceforth specified as material B) was 19 μm. Specimens for tensile testing were cut from 1.5 and 2.0 mm thick rolled metal sheets, of coarse grained and conventional material, respectively, using electro-discharge machining (EDM) with the gauge direction parallel to the rolling direction. Tensile elongation was performed at constant crosshead speed at temperatures between 300 and 520 °C and at strain rates between 10^{-3} and 10^{-1} s^{-1} in an HTE Hounsfield 5000E testing facility equipped with a retractable single zone furnace. The facility was positioned horizontally and the temperature of the furnace increased to the prescribed value within 5 minutes. Prior to straining, the system was allowed to reach a relative stability for a time interval of 5 minutes and then the specimens were extended to the point of failure. Upon failure the furnace was immediately retracted and the specimen was quenched in a water bath.

Stress strain curves were obtained using a video extensometer and the strain distributions over the gauge length were determined from optical measurements of the cross-sectional area of the gauge of the deformed specimens. The specimen surfaces were prepared for EBSD by conventional grinding, polishing according to the Struers method and final polishing using OP-U colloidal silica suspension with a particle diameter of 0.05 μm. EBSD was performed on a Philips XL-30 SEM operating at 30 kV, equipped with a fluorescent screen and manipulated by the TSL – EDAX application.

3 Results and discussion

3.1 Precipitates in the as-received microstructure

Fig. 1(a) and (b) show the microstructure of the as-received material C and B, respectively.

Fig. 2(a) shows some representative precipitates randomly positioned in the microstructure of the as-received material and Fig 2 (b) shows the EDX line-scan analyses performed indicating that these precipitates were relatively rich in Fe, Cu and Mn and deficient in Al and Mg. Two of these precipitates appear also relatively rich in Si. Similar analysis performed on the four precipitates in the as-received microstructure of the material B (shown in Fig. 2(c)) revealed similar results, i.e. two of the precipitates where rich in Fe, Cu, and Mn (those on the left) whereas the other two relatively rich in Si. A slight deficiency in Mg can be discerned for the first two precipitates but all four revealed an approximately equal Al content with that of the matrix.

3.2 Mechanical properties

Fig 3(a)-(b) shows the values of maximum elongation to failure for the coarse-grained (C) and the conventional (material B) AA5182. These were 220 and 200 %, respectively at 450 °C and at strain rate 10^{-2} s^{-1}. At 10^{-1} s^{-1} material C exceeded a 210 % elongation at temperatures between 480 and 500 °C and at 10^{-3} showed an appreciable elongation of 200 % at 350 °C. The conventional material performed rather poorly at these conditions.

Representative true stress – nominal strain curves at 450 °C for the material C and B are shown in *Fig. 4*(a) and (b), respectively. Excluding only the deformation of material C at 450 °C and at 10^{-2} s^{-1} all other curves exhibited an initial increase of the true stress followed by distinctive softening within the strain interval of 0.05 to 0.1, indicative of a low initial density of mobile dislocations which was followed by dislocation multiplication processes and cross-slip [10]. Only at 10^{-3} s^{-1}, for both materials, did the stress reach an appreciable plateau for a significant period during straining. At 10^{-1} s^{-1}, the stress more or less decreased steadily until the specimen's failure.

The variation of the maximum true stress as a function of strain rate for both materials is depicted in *Fig. 5*(a) and (b). For the temperatures used in this study and at the initial stages of deformation the stress and strain rate have a power law relationship, i.e. $\sigma \propto \dot{\varepsilon}^m$, where m is the strain rate sensitivity. This relationship is valid for the entire spectrum of temperatures and strain rates investigated (from 300 to 520 °C and from 10^{-3} to 10^{-1} s^{-1}). Here the values of true stress were taken at a nominal strain between 0.05 and 0.1. It is rather surprising that the strain rate sensitivity values for the coarse-grained material (C) lay systematically below 0.3 (with an average of 0.25). Only for the conventional material (B) did the strain rate sensitivity reach appreciably close to that of 0.3 (average value of ≈ 0.28) indicative of the solute drag creep mechanism [8]. The relatively low values of m, or the high value of the stress exponent $n = 1/m$ (which controls the dislocation velocity via the relationship $\upsilon \propto \sigma^n$) seems to indicate that the dis-

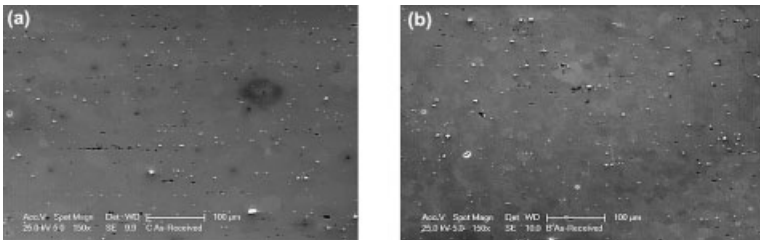

Fig. 1. (a) SEM image of the as received microstructure of the material C and (b) of B.

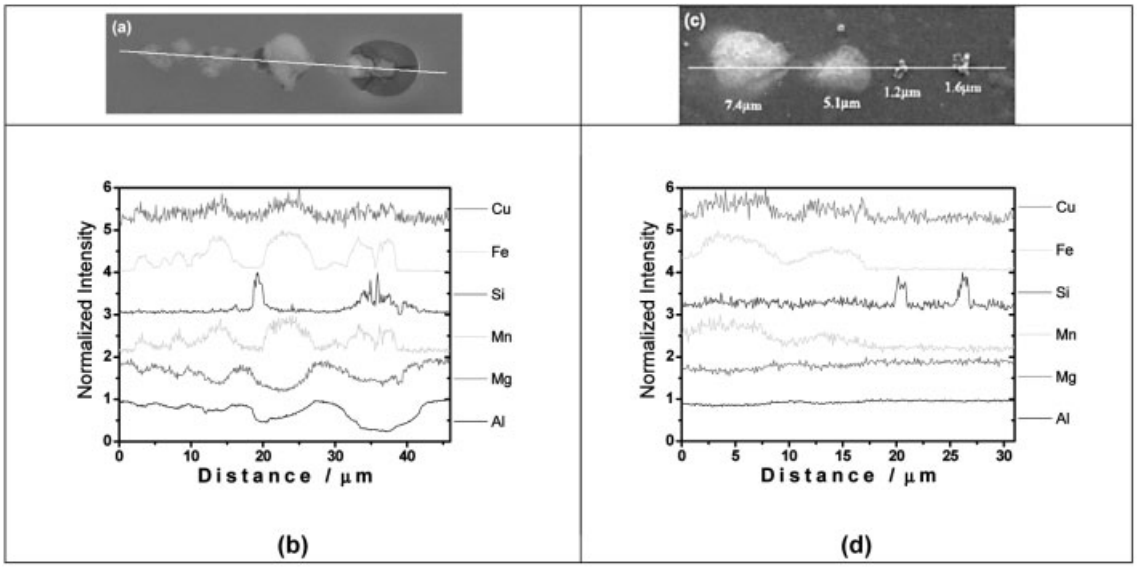

Fig. 2. (a) – (b) line scan EDX analysis on four precipitates observed in the as-received microstructure of material C and (c) – (d) similar analysis for the material B

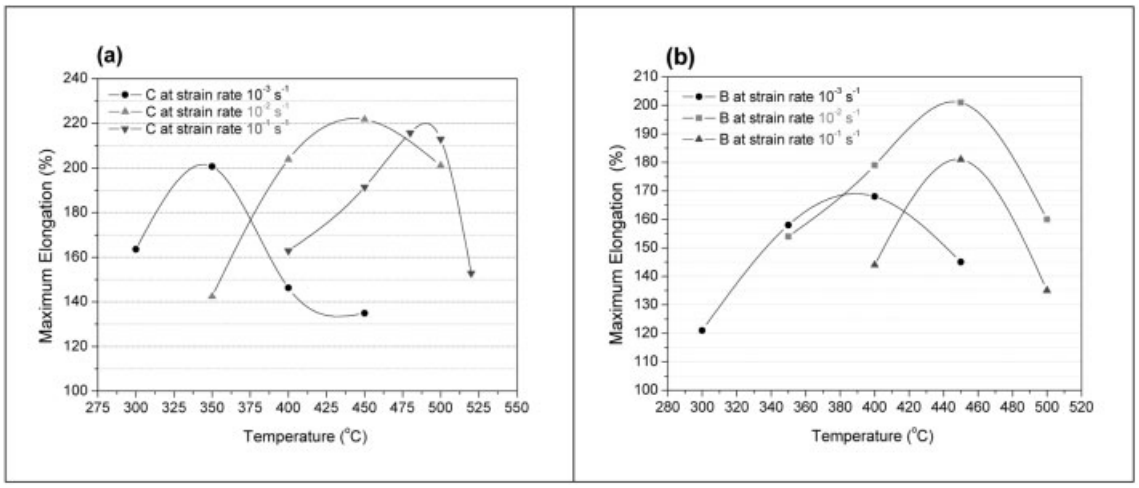

Fig. 3. Maximum elongation to failure for AA5182: (a) material C and (b) material B

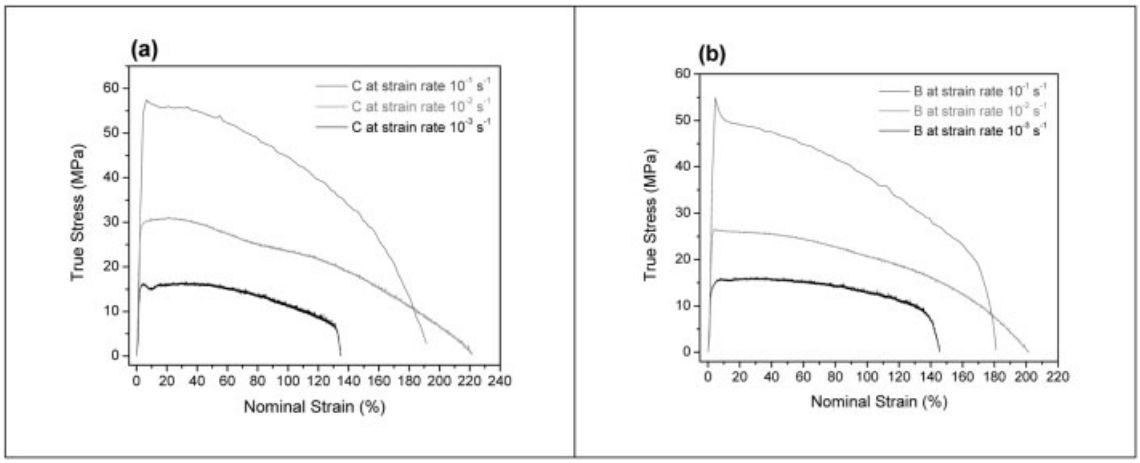

Fig. 4. Representative true stress – nominal strain curves at 450 °C for (a) the material C and (b) B.

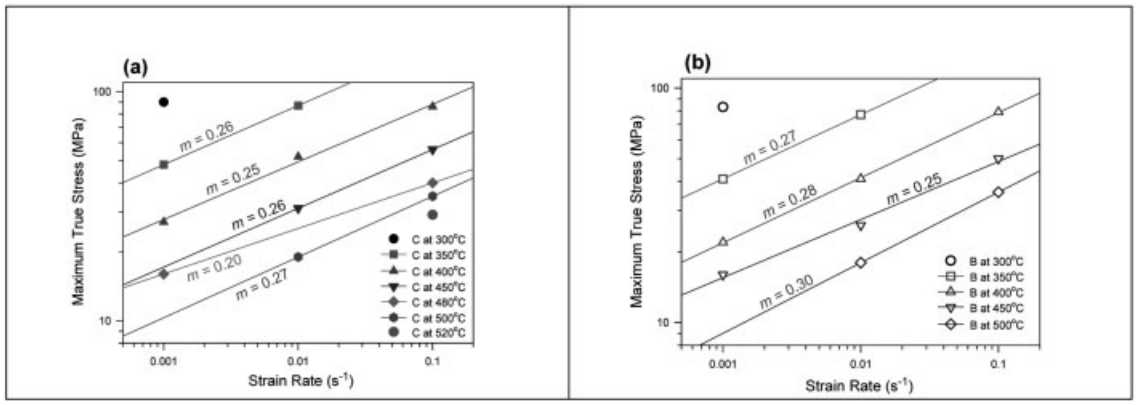

Fig. 5. Temperature dependence of the maximum true (flow) stress as a function of strain rate for the material C (a) and B (b).

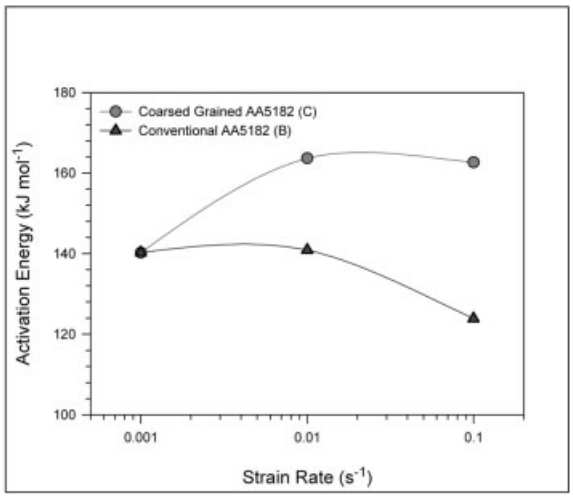

Fig. 6. Variation of the activation energy with the applied strain rate for the coarse-grained and the conventional AA5182.

location velocity is unusually of high at the first stages the deformation of the coarse-grained AA5182, i.e. the presence of the precipitates is unsuccessful in the formation and/or pinning the subgrain boundaries during the deformation of the material. The variation of the activation energy as a function of strain rate for both materials is depicted in *Fig. 6*. It varies, from 140 kJ mol^{-1}, at 10^{-3} and for the material C, it increased for higher strain rates to values slightly above 160 kJ mol^{-1}, whereas for the material B it dropped to a value close to 120 kJ mol^{-1} at the highest strain rate, which is lower than that of diffusion of Mg in Al (136 kJ mol^{-1}) [8]. This most probably occurred due to extensive diffusion of vacancies along the grain boundaries resulting to grain boundary migration at the onset of plastic deformation.

3.3 Microstructure evolution

The examination of the gauge section after deformation for both materials showed distinctive changes in the average grain size, high angle, low angle and sub-grain boundary fraction values, as well as the grain orientation in regions as one proceeds from the grips towards the tip of the failed specimens. *Fig. 7*(a) shows the specimen from material C, which failed at 220 % nominal strain at 450 °C and at 10^{-2} s^{-1}. Similarly Fig 7(b) shows the specimen of material B, which failed at 200 % nominal strain and at the same testing conditions. The first specimen failed approximately in the middle, whereas for the second the point of failure was located slightly towards the left (as seen in the figure). EBSD performed across the gauge revealed the grain size variation depicted in Fig 7(b) and (d), for the specimen from material C and B, respectively. The outermost data points (on the left and on the right of each diagram) correspond to the average grain size in the as-received microstructure (i.e. 34 and 19 μm, for C and B, respectively). The data points immediately next to them (the second from the left and the eigth) correspond to the grain size change sustained at the grips during heating up, stabilization and testing. It is obvious from the photographs that no deformation occurred at the grips. The microstructure of the coarse grained AA5182 is quite stable at the testing temperature, whereas that of the conventional material (B) sustained coarsening (i.e. increased to 21 μm). The third and the seventh data points in both diagrams correspond to sections of the gauge where "uniform deformation" was observed. The grain size of specimen from material C increased marginally to 36 μm, but that from material B coarsened significantly, presumably due to the residual stress stored on the material during fabrication, as well as the stress during deformation. Next to them lay the points corresponding to the "heavily deformed" region of the specimens where necking started to form. The average grain size of the specimen from material C remained constant with respect to that at the "uniformly deformed" region of the gauge, but that of the specimen from material B coarsened so much that its average value exceeded that of material C (i.e. 37 μm). In

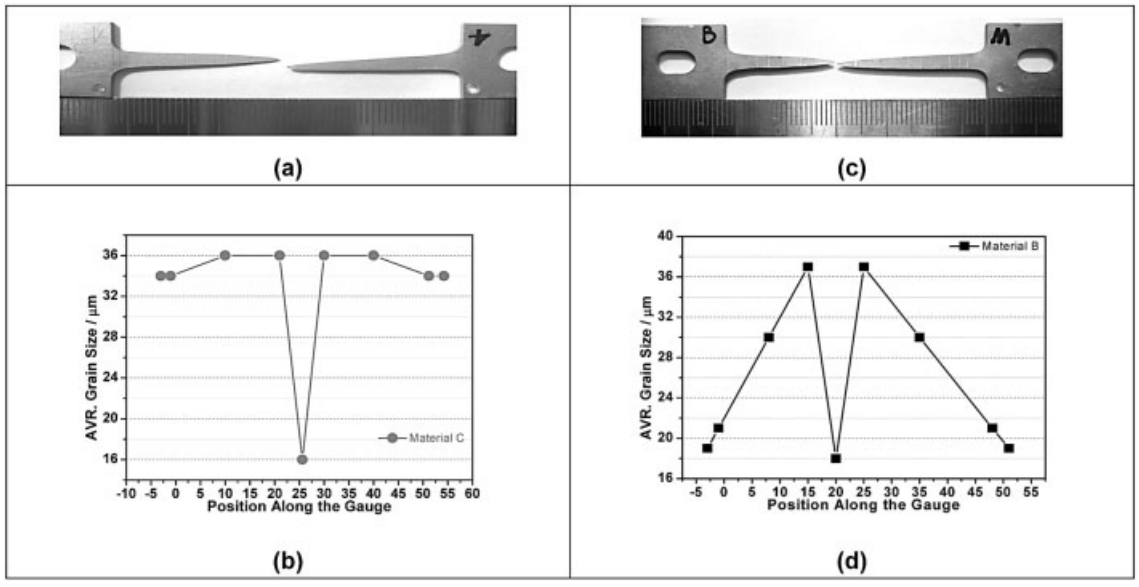

Fig. 7. (a) Deformed specimen of material C; (b) the values of the average grain size measured in various positions of the gauge from the grips to the tip; (c) deformed specimen of material B and (d) the average grain size measured in various positions in the gauge from the grips to the tip.

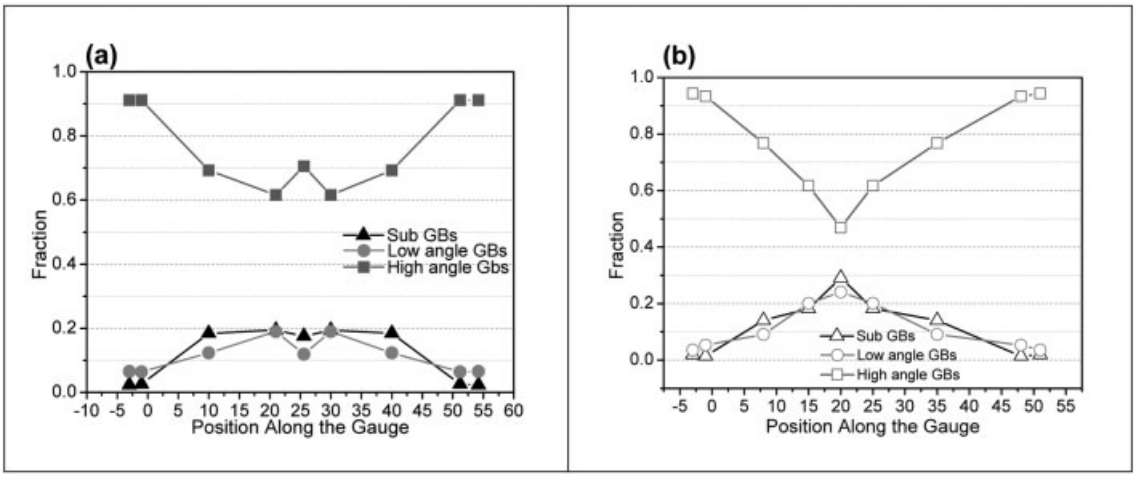

Fig. 8. The fraction of the subgrain boundaries, low angle grain boundaries and high angle grain boundaries as they were measured in various positions along the gauge (a) for the material C and (b) fro the material B.

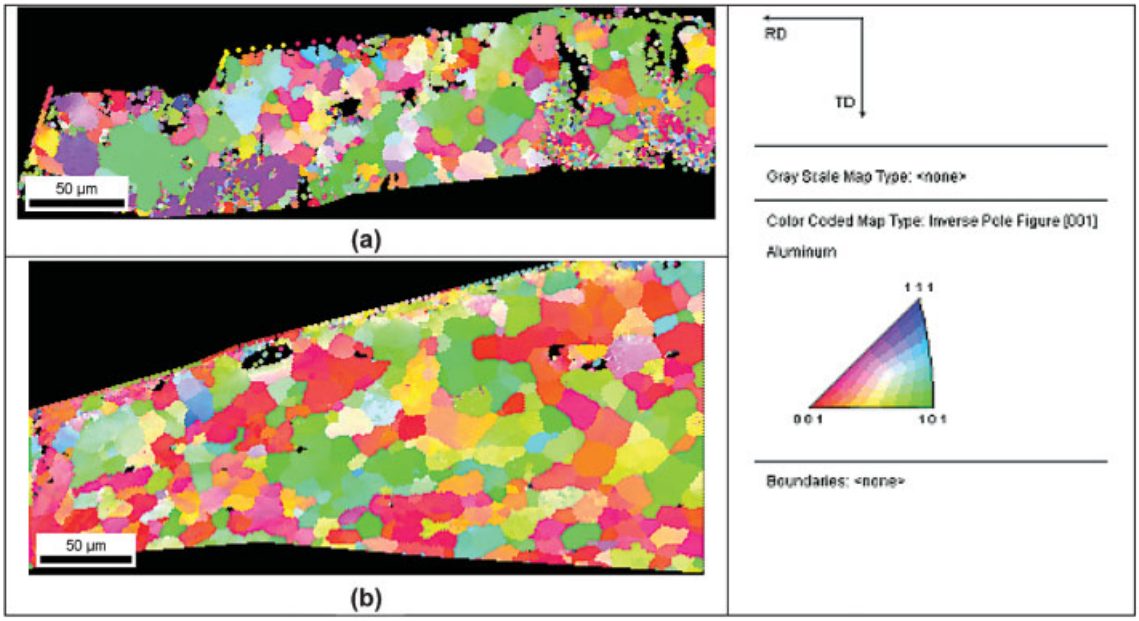

Fig. 9. Auto Inverse Pole figure obtained from the tip region of (a) the material C and (b) the material B along with the color coded map.

the region of the "tip" extensive recovery took place in the form of grain refinement and the average grain size decreased to 16 and 17 µm, for the material C and B, respectively.

The fraction of the subgrain boundaries, low angle grain boundaries and high angle grain boundaries, as they were measured in the as-received, heat treated, uniformly deformed, heavily deformed, and the microstructure at the tip is depicted in *Fig. 8*(a) and (b), for the specimens from material C and B, respectively. Progressing towards the tip, the fraction of high angle grain boundaries decreases, whereas that of low angle grain boundaries and subgrain boundaries increased. In material C, this situation was reversed at the tip where dynamic recrystallization occurred.

Fig. 9(a) and (b) depict the auto inverse pole figure at the tip of the specimens from material C and B, respectively. Extensive recovery has taken place in the form of grain refinement in both specimens. The material C (Fig. 9(a)) shows coarsening of a couple grains, probably evidence of dynamic recrystallization occurring exactly at the tip.

The low value of the strain rate sensitivity, suggests that the velocity of the mobile dislocation is high. The variation of the average grain size, as well as the fraction of the subgrain, low angle and high angle grain boundaries, along the gauge show that even though initially the material along the entire length of the gauge began to deform, a significant portion of the gauge remained unaffected as the neck instability developed. As soon as that occurred the stress concentration forced all the desirable mechanisms (recovery and reconstruction by subgrain boundary evolution into primarily low grain boundaries) to take place entirely in the necking region, whereas the material in the rest of the gauge did not contribute to the plasticity. This most likely occurred because the size and distribution of the precipitates is not capable to pin sufficiently the subgrain boundaries. Thus, the conversion of the subgrain

boundaries into low angle and/or high angle grain boundaries resulting in grain size reduction and microstructure refinement does not take place along the entire gauge. As a result the material AA5182, in its existent form exhibits poor superplasticity with maximum elongation not exceeding 220 %.

The behavior of the material at the tip indicates that the mechanism desired for superplastic deformation can take place in the alloy AA5182 (coarse grained and conventional alike). It is suggested, therefore, a fabrication method which will be able to introduce a large number of fine (submicron sized) precipitates will most probably be more effective in the subgrain boundary pinning. This will enable the material, along the entire length of the gauge, to contribute successfully in the deformation rendering the AA5182 appreciably superplastic.

4 Conclusions

- The coarse-grained Al alloy AA5182 exhibits poor superplasticity with a maximum elongation to failure not exceeding 220 % at 450 °C and at 10^{-2} s^{-1}.
- The low values of the strain rate sensitivity indicate that the dislocation velocity is quite high and necking is developed quite soon during deformation.
- The size (often exceeding 1 μm) and the distribution of the precipitates render them incapable of pinning the subgrain boundaries efficiently.
- As a result recovery and reconstruction by grain refinement occurs only within the necking region where the applied stress is concentrated.
- A fabrication method which will be able to introduce a large number of submicron sized precipitates will most likely result in sufficient pinning of the subgrain boundaries.
- This will promote recovery and reconstruction to take place more uniformly in the material rendering it appreciably superplastic.

5 References

1. SJ Hales, TR McNelly, *Acta Metall* **1988**, *36*, 1229.
2. OD Sherby, J. Wadsorth, *Prog Mater Sci* **1989**, *33*, 169.
3. MA Kulas, WP Green, EM Taleff, PE Krajewski, TR McNelly, *Metall Mater Trans A* **2005**, *36*, 1249.
4. ME Kassner, MT Pérez-Prado, *Prog Mater Sci* **2000**, *45*, 1.
5. AR Chezan, JTM De Hosson, *Mater Sci Forum* **2005**, 495–497, 883.
6. EM Taleff, GA Henshall, TG Nieh, DR Leseur, J. Wadsworth, *Metall Mater Trans A* **1998**, *29*, 1081.
7. SS Woo, YR Kim, DH Shin, WJ Kim, *Scripta Mater* **1997**, *37*, 1351.
8. OD Sherby, EM Taleff, *Mat Sci Eng A* **2002**, *322*, 89.
9. WA Soer, AR Chezan, JTM De Hosson, *Acta Mat* **2006**, *54*, 3827.
10. GA Henshall, ME Kassner, McQueen, *Metall Mater Trans A* **1997**, *23*, 936.

Corresponding author: Prof. dr. J.Th.M. De Hosson, Department of Applied Physics, Netherlands Institute for Materials Research, University of Groningen, Nijenborgh 4, 9747 AG Groningen, The Netherlands, E-mail address: j.t.m.de.hosson@rug.nl

Received in final form: January 31, 2008 [T 289]